Int. J. Heat Mass Transfer. Vol. 36, No. 8, pp. 2013–2020, 1993
Printed in Great Britain

0017–9310/93 $6.00+0.00

Local heat/mass transfer distribution in a square channel with full and V-shaped ribs

R. T. KUKREJA, S. C. LAU and R. D. McMILLIN
Department of Mechanical Engineering, Texas A&M University, College Station, TX 77843-3123, U.S.A.

(*Received* 24 *April* 1992 *and in final form* 10 *November* 1992)

Abstract—Naphthalene sublimation experiments have been conducted to study the turbulent heat/mass transfer characteristics of airflow in a square channel, in which two opposite walls are roughened with aligned arrays of full ribs and V-shaped ribs. The detailed distributions of the local heat/mass transfer coefficient on the ribbed walls and on the smooth walls are obtained. Results show that there are significant spanwise as well as streamwise variations of the local heat/mass transfer coefficient on the exposed surfaces of the ribbed walls in the oblique full rib and V-shaped rib cases.

INTRODUCTION

TO INCREASE the thermal efficiency of a gas turbine engine, a high gas entry temperature is desirable. For the internal components in the engine such as the blades to withstand the intense heat flux from the hot gases and the buildup of thermal stresses, an effective cooling system is required. The system must be able to maintain the temperatures in the walls of the blades relatively low and as uniform as possible, since excessive temperature variation may also shorten the designed life of the blades.

While the blade of a typical modern gas turbine is cooled externally by the ejection of air from the compressor through film cooling holes, compressed air is also circulated through internal straight or multipass shaped passages. To enhance the heat transfer to the cooling air, turbulence promoters (ribs) are cast onto the cooling passage walls whose outer surfaces are directly exposed to the hot gases. Researchers have modeled the internal cooling passages of turbine blades as rectangular channels with turbulence promoters on two opposite walls. A survey of the literature reveals that a number of researchers have conducted experiments to study how the geometry of turbulence promoters affects the rate of heat transfer and the streamwise pressure drop for the flow of a fluid through a channel. Examples of published work are Burggraf [1], Webb *et al.* [2], Lau *et al.* [3] and Han *et al.* [4].

These earlier studies give the overall heat transfer and thermal performances of various rib configurations on two opposite walls of rectangular channels. None of these studies, however, examined how varying the rib configuration alters the local heat transfer distribution and the fluid flow pattern. The detailed distributions of the local heat transfer coefficient in rib-roughened channels are important because they enable a turbine engine designer to calculate the local temperature distributions in turbine blades under actual operating conditions and to identify the locations of high thermal stresses. The detailed local distributions are also needed by a designer to formulate new analytical or numerical models to optimize the configurations of the ribs on internal coolant passages in turbine blades for best thermal performance, and to predict the local temperatures and local convective heat transfer for flows through these shaped coolant passages.

The task to determine the detailed local heat transfer distribution in a rib-roughened channel by conducting heat transfer experiments is arduous because of problems associated with local temperature and heat flux measurements, extraneous heat losses, and conduction along the channel walls. The shortcomings of conventional heat transfer techniques forced some researchers to explore other methods to determine the local distributions of heat transfer coefficient, among them is the naphthalene sublimation mass transfer technique. The boundary condition on a naphthalene surface is analogous to that of uniform wall temperature in a corresponding heat transfer experiment. Naphthalene sublimation experiments do not have the problems which correspond to extraneous heat losses through thermal insulation and conduction along channel walls, and are relatively inexpensive to conduct. Finally, the naphthalene sublimation technique offers high measurement resolution and the flexibility of determining the local mass transfer coefficients at as many points as needed on a naphthalene surface. By applying the analogy between heat and mass transfer, the local distribution of the heat transfer coefficient may be determined from the mass transfer coefficient distribution [5].

The objective of this investigation is to study the local heat/mass transfer characteristics of 'periodically' fully developed turbulent flow of air in a

NOMENCLATURE

D	hydraulic diameter of channel [m]
e	rib height [m]
h_m	local mass transfer coefficient, $\dot{m}''/(\rho_w-\rho_b)$ [m s^{-1}]
$\dot{m}$	total mass flow rate of air [kg s^{-1}]
$\dot{m}''$	mass diffusion flux of naphthalene, $\rho_s(\Delta z/\Delta t)$ [kg m^{-2} s^{-1}]
p	rib pitch [m]
Re_D	Reynolds number based on hydraulic diameter and average velocity, $\dot{m}/(D\mu)$
s	spacing between adjacent measurement lines [m]
Sc	Schmidt number, ν/σ, 2.5 for naphthalene in air
Sh_D	local Sherwood number, h_mD/σ
$\overline{Sh}_D$	spanwise average Sherwood number
Sh_0	Sherwood number for fully developed flow through a smooth channel, given by the Dittus–Boelter equation, $0.023\,Re_D^{0.8}\,Sc^{0.4}$
x	streamwise distance from upstream face of a rib or rib segment [m]
y	distance along axis of a rib or rib segment [m].

Greek symbols

Δt	duration of test run [s]
Δz	change of elevation at measurement point on naphthalene surface [m]
μ	dynamic viscosity of air [N s m^{-2}]
ν	kinematic viscosity of air [m^2 s^{-1}]
ρ_b	bulk vapor density of naphthalene [kg m^{-3}]
ρ_s	density of solid naphthalene [kg m^{-3}]
ρ_w	local vapor density of naphthalene at surface [kg m^{-3}]
σ	diffusion coefficient [m^2 s^{-1}].

square channel with full ribs and V-shaped ribs on two opposite walls. Naphthalene sublimation experiments are performed to determine the detailed distributions of the local heat/mass transfer coefficient on the ribbed walls and the smooth walls for full rib and V-shaped rib configurations with various rib angles-of-attack. From the local results, the flow patterns over various arrays of transverse full ribs, angled full ribs, and V-shaped ribs are compared. It is also of interest to obtain the relative contributions of the heat/mass transfer from the rib surfaces and that from the exposed surfaces of the ribbed walls to the overall heat/mass transfer from the ribbed walls.

EXPERIMENTAL APPARATUS AND PROCEDURE

The test apparatus is an open air flow loop in an air-conditioned laboratory. The test section is a square channel with two opposite naphthalene-coated rib-roughened walls and two naphthalene-coated smooth walls. It has a flow cross section of 7.62 × 7.62 cm and a length of 0.38 m. Each wall is constructed from a 6.35 mm thick aluminum plate. The bottom wall consists of four segments that are aligned end to end in the streamwise direction (Fig. 1(a)). One of the segments is 19.1 cm long; one 9.53 cm long; and two 4.76 cm long. The segments are attached with flat head machine screws onto a 0.38 m long, 3.18 mm thick support plate.

The inner half of each of the channel walls and wall segments is a rectangular, 3.18 mm thick layer of naphthalene that is surrounded on its four sides by a rim (or a rectangular cavity with a thin rim filled with naphthalene). Thus, except for the top of the rims, the exposed surfaces of the four channel walls are mass transfer active (see Fig. 1(a)). The naphthalene 'coating' on each wall or wall segment is prepared in a casting process such that the exposed naphthalene surface is as smooth and flat as a highly-polished stainless steel plate used in the casting process.

The top and bottom walls of the test section are roughened with rib turbulators and the two vertical side walls are smooth. Ribs are attached with silicone rubber adhesive onto the interior surfaces of the top and bottom walls at fixed intervals along the streamwise direction. The rib configurations that are of interest are transverse full ribs, 60° angled full ribs, and 45°, 60°, and 135° V-shaped ribs (Fig. 1(b)).

The ribs are cut from 0.48 × 0.48 cm square balsa wood. Therefore, the rib height-to-hydraulic diameter ratio, e/D, in this study is 0.0625. By applying molten naphthalene with a brush onto the exposed surfaces of the ribs and allowing it to solidify, the ribs are coated with a thin layer of naphthalene, and the exposed surfaces of the ribs are mass transfer active during an experiment. For experiments to determine the mass transfer from the exposed surfaces of the ribs, all of the ribs (or rib segments) are prepared by casting, and are attached with double-sided adhesive tape onto the channel walls.

The four walls of the test section are designed such that the test section may be assembled quickly by matching the edges of the four walls and by tightening several flat head machine screws. During an experiment, adhesive tape is used over the joints between adjacent walls and over the screws to prevent air leakage.

The test section is mated to a 0.76 m long entrance

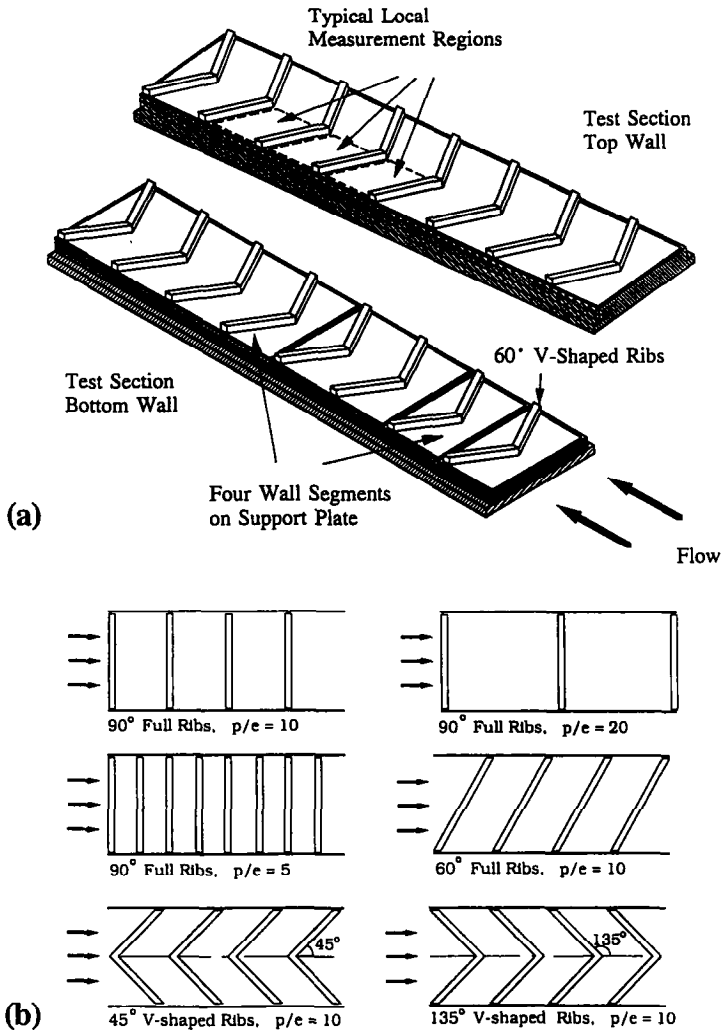

FIG. 1. (a) Schematic of test section; (b) typical rib configurations.

section at the upstream end and an exit duct at the downstream end with matching flanges and machine screws. Both the entrance section and the exit duct have the same flow cross section as the test section but have four smooth walls. During an experiment, the mixture of air and naphthalene vapor leaving the test flow loop is ducted into a fume hood, where the mixture is drawn to the outside of the building with an exhaust fan.

The instrumentation, the experimental procedure, the data reduction method, and the experimental uncertainties are given in detail in a Ph.D. dissertation by Kukreja [6] and are not repeated here.

PRESENTATION AND DISCUSSION OF RESULTS

In each of the cases studied, the local Sh_D/Sh_0 distribution is based on measurements over a region between two consecutive ribs (or rib segments) on a wall several rib pitches from the channel entrance, where the variation of Sh_D/Sh_0 may be considered periodic. Indeed, experimental results show that the differences among corresponding local distributions between two ribs over two to three consecutive regions on a wall far downstream of the test channel entrance (for instance, more than five rib pitches from the channel entrance in the $p/e = 10$ cases) are within the uncertainty of the results.

In the subsections that follow, the normalized local Sherwood number, Sh_D/Sh_0, on a ribbed wall is given as a function of x and y; x being the streamwise distance from the upstream face of the rib (or rib segment) located immediately upstream of the measurement region, and y being the distance along the axis of a rib (or rib segment) measured from a smooth wall or from the upstream end of an angled rib (or rib segment). In the transverse full rib cases, the spanwise variations of Sh_D/Sh_0 are generally small. A normalized spanwise average Sherwood number, $\overline{Sh}_D/Sh_0$, is defined and is given as a function of x only. In the V-shaped rib cases, due to geometric

symmetry, it is necessary to present the local Sh_D/Sh_0 distributions in one-half of the region between two consecutive ribs only.

Attention is focused here on the local Sh_D/Sh_0 distributions on the ribbed walls. The local Sh_D/Sh_0 distributions on the smooth walls are not presented here, although they are also determined in this study. Interested readers are referred to Kukreja [6].

Transverse full ribs

Turbulent flow of a coolant over periodic transverse ribs on a wall may be characterized by flow separation on the top surface of a rib, a strong shear layer that results in flow recirculation immediately downstream of the rib, flow reattachment on the wall if the rib pitch is sufficiently large, the redevelopment of a boundary layer downstream of the reattachment region, and a relatively small recirculation zone upstream of the next downstream rib. As a result of flow impingement, the local heat transfer is expected to be high near the reattachment region. The local heat transfer must decrease as the thickness of the boundary layer downstream of reattachment increases. When the rib pitch is small, the flow does not reattach and the entire region between the two ribs is occupied by recirculating coolant. The local heat transfer is expected to be high near the downstream rib and decrease toward the upstream rib as the recirculating coolant washes the exposed wall in a reverse flow direction.

Figures 2(a)–(c) show the distributions of the normalized spanwise average Sherwood number, $\overline{Sh}_D/Sh_0$, on the exposed surface of a ribbed wall between two consecutive transverse ribs for $p/e = 10$, 20, and 5, and for $Re_D \cong 10\,000$ and 45 000. The values of $\overline{Sh}_D/Sh_0$ are based on those of Sh_D/Sh_0 that are obtained along 12 equally-spaced axial lines over one-half of the exposed surface between two ribs. In the figures, the distance from the upstream face of the upstream rib is normalized with the height of the rib, e, and square blocks indicate the locations of the two ribs.

In the $p/e = 10$ case (Fig. 2(a)), $\overline{Sh}_D/Sh_0$ decreases initially with increasing x/e, then increases and reaches a local maximum between $x/e = 4.0$ and 5.0, where the flow reattaches on the wall. The initial decrease of the local mass transfer suggests that there are two counter-rotating recirculation zones between the downstream face of the upstream rib and the reattachment region, with a smaller recirculation zone nearer the upstream rib. The local mass transfer then decreases gradually as the flow near the wall redevelops. The distribution has a local minimum at about one rib height upstream of the upstream face of the downstream rib, and an abrupt increase immediately upstream of the downstream rib. It is evident that some of the flow approaching the downstream rib is forced back, resulting in flow recirculation in a relatively small region immediately upstream of the downstream rib.

The two $\overline{Sh}_D/Sh_0$ distributions for $Re_D \cong 10\,000$ and 45 000 in Fig. 2(a) are similar except that there is less variation in the distribution for $Re_D \cong 45\,000$. The value of $\overline{Sh}_D/Sh_0$ in the higher Re_D case is generally higher near the two ribs but lower around the local maximum (at $x/e \cong 4.5$).

The two distributions in the $p/e = 20$ case that are shown in Fig. 2(b) have similar shapes and exhibit the same trend as those for $p/e = 10$. The local maxima occur between $x/e = 5.0$ and 6.0, about one rib height downstream of those in the $p/e = 10$ case. Along each distribution for $p/e = 20$, as the flow redevelops after reattachement, the long, uninterrupted gradual drop of $\overline{Sh}_D/Sh_0$ between $x/e \cong 6.0$ and 18.5 results in a local minimum value of $\overline{Sh}_D/Sh_0$ that is smaller than the corresponding value for $p/e = 10$. The values of $\overline{Sh}_D/Sh_0$ in the $Re_D \cong 45\,000$ case are generally higher near the two ribs again but are lower over most of the exposed wall than those in the $Re_D \cong 10\,000$ case.

The $\overline{Sh}_D/Sh_0$ distributions for $p/e = 5$ in Fig. 2(c) have local minima near the upstream rib between $x/e = 1.0$ and 2.0, and increase monotonically toward the downstream rib. It may be concluded that the flow does not reattach on the wall, and two counter-rotating pockets of recirculating air fill the space between the two ribs: a large pocket of air that occupies almost the entire space between the two ribs, and a small pocket of air near the upstream rib. The two distributions for $p/e = 5$ have similar shapes with generally smaller variation in the higher Re_D case.

60° full ribs

When two opposite walls of a square channel are roughened with parallel angled full ribs, the flow near each of the ribbed walls is three-dimensional, as oblique secondary flows caused by the ribs interact with the main flow over the ribbed wall. In the case that the rib pitch is sufficiently large that the main flow reattaches on the exposed channel wall, secondary flows may affect the recirculation of the flow near the upstream and downstream faces of the ribs, and may interrupt the growth of the boundary layers downstream of the reattachment regions.

In this study, the local mass transfer distributions on the exposed surface of the wall between two consecutive 60° full ribs are determined for two values of Re_D with a uniform measurement grid of 11×25: 25 points along 11 lines parallel to the main flow direction. The lines are equally-spaced and are located at $y/s = 0.5$, 1.5, 2.5, 3.5, ..., and 10.5, y being the distance along the axis of a rib measured from the end of the rib nearer the channel entrance, and s the spacing between two lines along y and is equal to 1/11 of the length of a rib. Figures 3(a) and (b) give the local results as the streamwise distributions of the normalized local Sherwood number, Sh_D/Sh_0, along the eleven lines, for $Re_D \cong 10\,000$ and 45 000, respectively.

The local distributions show significant spanwise variation. The local Sherwood number generally decreases with increasing y/s and is higher in the lower

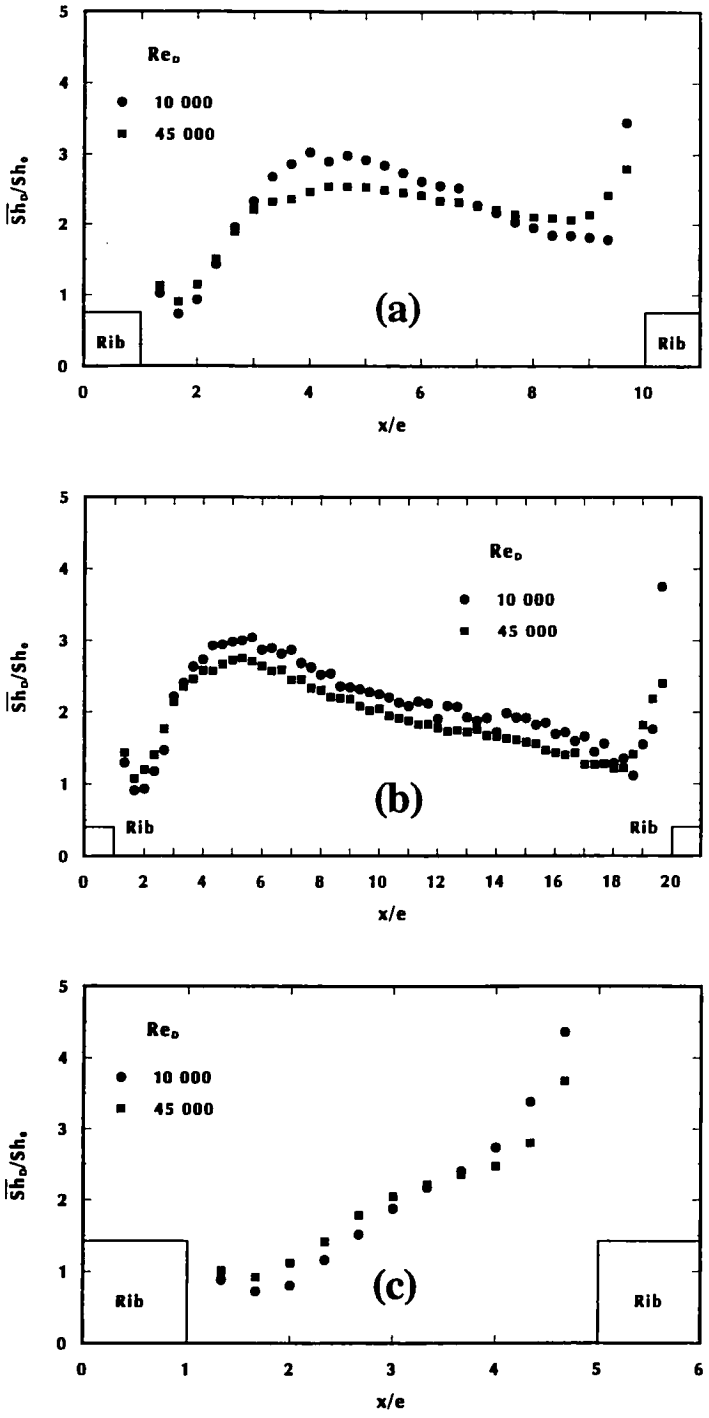

FIG. 2. Ribbed wall $\overline{Sh}_D/Sh_0$ distributions, 90° full ribs, (a) $p/e = 10$; (b) $p/e = 20$; (c) $p/e = 5$.

Re_D case. Along the line at $y/s = 0.5$, the value of Sh_D/Sh_0 increases to a maximum as the flow reattaches and then decreases gradually as the flow redevelops. The high mass transfer immediately upstream of the downstream rib indicates that there is flow recirculation immediately upstream of the downstream rib. Thus, the Sh_D/Sh_0 distributions along $y/s = 0.5$ are similar to those in the transverse rib cases. The values of Sh_D/Sh_0 in the reattachment regions, however, are much higher than those in the transverse rib cases. Also, the distributions show that the flow near the smooth wall at $y/s = 0.0$ in the $Re_D \cong 45\,000$ case reattaches 'earlier' than in the $Re_D \cong 10\,000$ case and in the transverse rib cases.

The distributions along the next several lines are similar to those along $y/s = 0.5$ except that the value

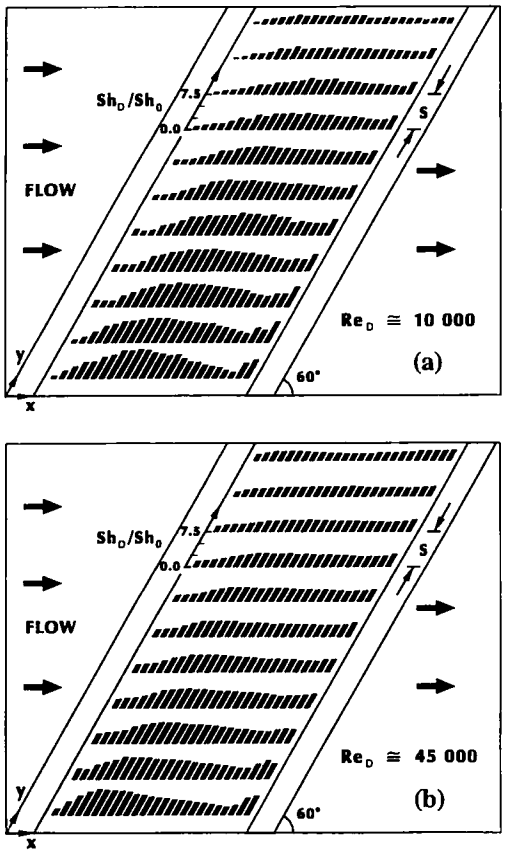

FIG. 3. Ribbed wall Sh_D/Sh_0 distributions, 60° full ribs. $p/e = 10$, (a) $Re_D \cong 10\,000$; (b) $Re_D \cong 45\,000$.

of Sh_D/Sh_0 along a line is lower in the flow reattachment region and is higher as the flow redevelops. As y/s increases, the value of the local maximum decreases while that of the local minimum increases, as secondary flows caused by the angled ribs interrupt flow reattachment and boundary layer redevelopment on the exposed channel wall between the two ribs.

Along the lines at $y/s \geqslant 5.5$, the local Sherwood number decreases further with increasing y/s as secondary flows wash the exposed wall in an oblique direction relative to that of the main flow. The impingement of the flow on the wall in the reattachment region is much weaker, resulting in a lower rate of local mass transfer, and there is only a very small drop of Sh_D/Sh_0 following flow reattachment.

60° V-shaped ribs

When two opposite walls of a square channel are roughened with 60° V-shaped ribs, the rib segments divert the flows near the ribbed walls toward the two smooth walls. These secondary flows interact with the main flow over the ribbed walls, affect flow reattachment and recirculation between consecutive rib segments, and interrupt boundary layer growth downstream of the reattachment regions.

The local mass transfer distributions on one half of the exposed surface of a ribbed wall between two 60° V-shaped ribs are determined for two values of Re_D with a uniform measurement grid of $12 \times 25 : 25$ points along 12 equally-spaced axial lines located at $y/s = 0.0, 1.0, 2.0, 3.0, \ldots$, and 11.0. The coordinate y is the distance along the axis of a rib segment measured from the end of the rib segment nearer the channel entrance, and s is the spacing between two lines along y and is equal to 2/23 of a rib segment. Figures 4(a) and (b) give the streamwise distributions of the normalized local Sherwood number, Sh_D/Sh_0, along the twelve lines. The figures are for $Re_D \cong 10\,000$ and 45 000, respectively.

The local distributions in Figs. 4(a) and (b) show significant spanwise variation as well as streamwise variation, as in the 60° full rib case, and have some of the features of the 60° full rib distributions. In each figure, a region of low mass transfer immediately downstream of the upstream rib segment indicates flow recirculation, which extends further from the upstream rib nearer the middle of the wall. The larger recirculating zone in the middle of the wall in the lower Re_D case is especially evident. The local distribution is generally lower for a larger value of y/s in both $Re_D \cong 10\,000$ and 45 000 cases. Thus, it appears that oblique secondary flows originate in the middle of the ribbed wall and move along the exposed surface of the wall toward the two smooth walls.

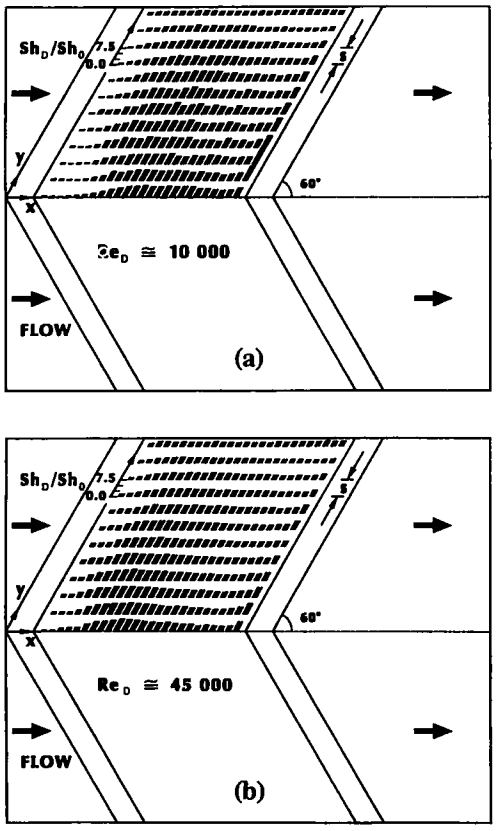

FIG. 4. Ribbed wall Sh_D/Sh_0 distributions, 60° V-shaped ribs, $p/e = 10$, (a) $Re_D \cong 10\,000$; (b) $Re_D \cong 45\,000$.

Along the first several lines near $y/s = 0.0$, the value of Sh_D/Sh_0 increases to a maximum as the flow reattaches. The flow near the centerline of the ribbed wall (at $y/s = 0.0$) reattaches 'later' in the $Re_D \cong 10\,000$ case than in the $Re_D \cong 45\,000$ case. In each case, the flow near the centerline reattaches later than the flow near the smooth wall at $y/s = 0.0$ in the corresponding 60° full rib cases. While the value of Sh_D/Sh_0 decreases gradually as the flow redevelops, the drops in the distributions are less compared with those in the distributions near the smooth wall at $y/s = 0.0$ in the 60° full rib case. The differences between corresponding distributions may be attributed to the existence of the smooth wall at $y/s = 0.0$ in the 60° full rib case and the lack of one at $y/s = 0.0$ in the 60° V-shaped rib case.

As y/s increases, the value of Sh_D/Sh_0 in the flow reattachment region decreases. Secondary flows guided by the rib segments interrupt flow reattachment on the exposed channel wall and the impingement of the flow on the wall in the reattachment region is much weaker. There is only a very small drop of Sh_D/Sh_0 following flow reattachment. As in the 60° full rib case, the variation of Sh_D/Sh_0 is small along the distributions near the smooth wall at $y/s = 11.5$.

The Sh_D/Sh_0 distributions on a smooth wall in the V-60° rib case are very similar to, but higher than, those on the smooth wall at $y/s = 11.0$ in the 60° full rib case. The higher values may be attributed to the impingement on the smooth wall of the stronger oblique secondary flows that originate near the middle of the ribbed wall.

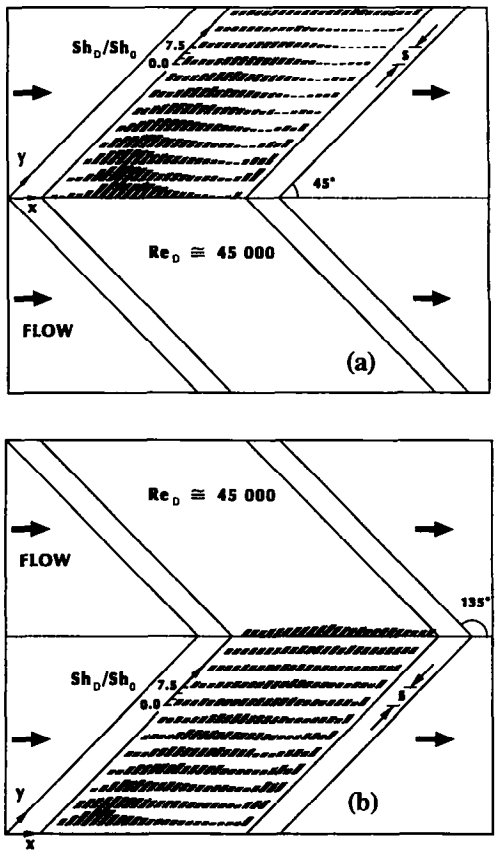

FIG. 5. Ribbed wall Sh_D/Sh_0 distributions, $p/e = 10$, $Re_D \cong 45\,000$, (a) 45° V-shaped ribs; (b) 135° V-shaped ribs.

45° and 135° V-shaped ribs

Figures 5(a) and (b) show the Sh_D/Sh_0 distributions along twelve axial lines for $Re_D \cong 45\,000$ in the 45° and 135° V-shaped rib cases, respectively. The variations of the local mass transfer on the exposed surface of the ribbed wall in the two cases differ significantly and are quite different from that for the 60° V-shaped ribs (see Fig. 4(b)). In the middle of the wall with the 45° V-shaped ribs (Fig. 5(a)), Sh_D/Sh_0 along $y/s = 0.0$ reaches a very high value at $x/e \cong 5.0$, and drops to a very low minimum as the flow reattaches and the downstream boundary layer redevelops. The variations of the several Sh_D/Sh_0 distributions near the middle of the ribbed wall are larger than those of corresponding distributions in the V-60° rib case: the maxima are higher and the minima are lower in the V-45° rib case. In the V-45° rib case, the flow near the middle of the wall reattaches nearer the upstream rib segment and the recirculation zone downstream of the upstream rib is smaller than that in the V-60° rib case. Upstream of the downstream rib segment, there is a large and wide region of very low mass transfer that is not evident in the Sh_D/Sh_0 distribution in the V-60° rib case. On the average, the mass transfer from the exposed surface of the ribbed wall is higher in the V-60° rib case than in the V-45° rib case.

In the V-135° rib case (Fig. 5(b)), the Sh_D/Sh_0 distribution along the line nearest the smooth wall resembles that along the first line from the smooth wall at $y/s = 0.0$ in the 60° full rib case (see Fig. 3(b)). In both cases, the flow moves away from the adjacent smooth wall. The flow reattaches early and the distribution drops to a very low value before rising immediately upstream of the downstream rib or rib segment.

Figure 5(b) shows that the variation of the local distribution is generally smaller for a larger value of y/s (that is, nearer the centerline of the ribbed wall). It appears that oblique secondary flows that originate near the smooth wall and move toward the middle of the ribbed wall weaken the reattachment of the main flow on the exposed surface of the wall between two rib segments.

The Sh_D/Sh_0 distribution along the centerline of the ribbed wall is slightly higher than those along the next two lines. If there are two large counter-rotating vortices in the flow near a ribbed wall, resulting from the interaction of the oblique secondary flows with the main flow, the Sh_D/Sh_0 distribution should continue to drop toward the middle of the ribbed wall. Thus, there may be a pair of smaller vortices in the flow near the middle of the ribbed wall rotating in

directions opposite to those of the two larger main vortices in the flow.

The Sh_D/Sh_0 distributions in the V-135° rib case generally do not vary as much as those in the V-45° rib case. There is not a large region of very low mass transfer on the exposed surface of the wall between two V-135° rib segments as in the V-45° rib case. The average mass transfer on the exposed surface of the ribbed wall is generally lower in the V-135° rib case than in the V-45° rib case.

The normalized regional average Sherwood numbers for the exposed surfaces of the ribbed walls and the smooth walls are determined from the local Sh_D/Sh_0 distribution over the measurement regions on the respective walls. The average Sherwood numbers for the exposed surfaces of the ribs, normalized with Sh_0, are obtained from the direct measurements of the overall rates of mass loss from the rib surfaces with a high-precision electronic balance. The average Sherwood numbers for the ribs are compared with the average ribbed wall and smooth wall Sherwood numbers.

The results show that the values of the average Sherwood number for the ribs are higher than those for the ribbed walls, which, in turn, are higher than those for the smooth walls. The regional average mass transfer results are consistent with published overall heat transfer results [3]: among the $p/e = 10$ cases, 60° V-shaped ribs cause the highest mass transfer from the ribbed walls and 90° full ribs cause the lowest mass transfer; the normalized ribbed wall Sherwood number decreases with increasing Reynolds number; and increasing the value of p/e from 10 to 20 lowers the mass transfer from the ribbed walls. The average mass transfer results also show that decreasing the value of p/e from 10 to 5 reduces the mass transfer from both the ribbed walls and the smooth walls. The regional average mass transfer results are available in detail in ref. [6].

CONCLUDING REMARKS

Based on the results of the study, the following conclusions are drawn:

(1) Secondary flows that are caused by oblique ribs (or rib segments) interact with the main flow over the ribbed walls, affect flow reattachment and recirculation between the ribs (or rib segments), and interrupt boundary layer growth downstream of the reattachment regions.

(2) In the angled rib cases, there are significant spanwise variations of the local mass transfer coefficient on the exposed surfaces of the ribbed walls.

(3) In the 45° and 60° V-shaped rib cases, secondary flows over the ribbed walls originate in the middle of the ribbed walls and move toward the two smooth walls. In the 135° V-shaped rib case, secondary flows originate near the smooth walls and move toward the middle of the ribbed walls.

(4) The variations of the local mass transfer coefficient on the exposed surfaces of the ribbed walls are generally much larger in the 45° V-shaped rib case than in the 60° V-shaped rib case.

(5) In the 60° full rib case, secondary flows over the ribbed walls move from one smooth wall toward the other smooth wall. The distributions of the local mass transfer coefficient on the two smooth walls are distinctly different.

(6) The average mass transfer coefficient on the ribs is higher than that on the exposed surfaces of the ribbed walls.

Acknowledgement—The authors appreciate the support of this research by the National Science Foundarion (grant no. CTS8910860).

REFERENCES

1. F. Burggraf, Experimental heat transfer and pressure drop with two-dimensional turbulence promoter applied to two opposite walls of a square tube. In *Augmentation of Convective Heat Mass Transfer* (Edited by A. E. Bergles and R. L. Webb), pp. 70–79. ASME, New York (1970).
2. R. L. Webb, E. R. G. Eckert and R. Goldstein, Heat transfer and friction in tubes with repeated rib-roughness, *Int. J. Heat Mass Transfer* **14**, 601–617 (1971).
3. S. C. Lau, R. T. Kukreja and R. D. McMillin, Effects of V-shaped rib arrays on turbulent heat transfer and friction of fully developed flow in a square channel, *Int. J. Heat Mass Transfer* **34**, 1605–1616 (1991).
4. J. C. Han, Y. M. Zhang and C. P. Lee, Influence of surface heat flux ratio on heat transfer augmentation in square channels with parallel, crossed and V-shaped angled ribs, ASME Paper 91-GT-3 (1991).
5. E. R. G. Eckert, Analogies to heat transfer processes. In *Measurements in Heat Transfer*, pp. 399–412. McGraw-Hill, New York (1976).
6. R. T. Kukreja, Turbulent heat/mass transfer enhancement with V-shaped ribs in a square channel, Ph.D. Thesis, Texas A&M University, College Station, Texas (1992).